small
NANO MICRO

Detection of Single DNA Molecule Hybridization on a Surface by Atomic Force Microscopy

*David Pastré, Vandana Joshi, Patrick A. Curmi, and Loic Hamon**

Improving the detection of DNA hybridization is a critical issue for several challenging applications encountered in microarray and biosensor domains. Herein, it is demonstrated that hybridization between complementary single-stranded DNA (ssDNA) molecules loosely adsorbed on a mica surface can be achieved thanks to fine-tuning of the composition of the hybridization buffer. Single-molecule DNA hybridization occurs in only a few minutes upon encounters of freely diffusing complementary strands on the mica surface. Interestingly, the specific hybridization between complementary ssDNA is not altered in the presence of large amounts of nonrelated DNA. The detection of single-molecule DNA hybridization events is performed by measuring the contour length of DNA in atomic force microscopy images. Besides the advantage provided by facilitated diffusion, which promotes hybridization between probes and targets on mica, the present approach also allows the detection of single isolated DNA duplexes and thus requires a very low amount of both probe and target molecules.

1. Introduction

Surface hybridization is the basis of numerous DNA technologies from microarrays used to evaluate gene expression or sequencing to biosensors with many applications in the fields of clinical, medico-legal, environmental, veterinary, and food industries.[1] In such applications, single-stranded nucleic acids tethered on a solid support, a planar surface,[2] or colloidal particles,[3] referred to as "probes", are used to capture complementary single-stranded DNA (ssDNA) or RNA molecules from solution, referred to as "targets". Typically, thousands of probes (short oligonucleotides or DNA) are immobilized on microscopic spots.[4] Then, the hybridization between probes and targets can be detected by different means based on optical,[5] electrochemical,[6] gravimetric,[7] or nanomechanical[8] detection schemes. The most prominent assays rely on fluorescence techniques, which require the chemical modification of target and/or probe sequences with dye tags before testing. The current detection limit of DNA target is between the nanomolar and the picomolar range,[9] and may reach femtomolar by using a typical design of DNA probe, such as a molecular beacon.[10]

The detection sensitivity of DNA microarrays or sensors is determined by the hybridization efficiency, that is, the ratio of probes that have captured a target and the amount of target captured.[11] One of the main factors affecting these parameters is the probe density on the surface[12] and the point is to find a compromise. Indeed, a high probe density is mandatory for high detection sensitivity and to avoid DNA lying flat on the surface, which generally inhibits hybridization. However, increasing probe density leads to a crowded interfacial environment characterized by nucleotide concentrations that approach the molar range and a high level of immobilized negative charges, both of which have a dramatic impact on probe accessibility to the target, the incubation time, and thus global efficiency of the device. To overcome such barriers, steric hindrance could be limited by coadsorbing lateral spacer molecules that impede the probe adsorption on the substrate.[13] Another possibility is to use nanostructured surfaces with small radius of curvature to space out the probes and increase

Prof. D. Pastré, V. Joshi, Dr. P. A. Curmi, Dr. L. Hamon
Inserm U829, Laboratoire Structure-Activité des Biomolécules Normales et Pathologiques
Université d'Evry-Val d'Essonne
Evry 91025, France
E-mail: loic.hamon@univ-evry.fr

DOI: 10.1002/smll.201300546

© 2013 Wiley-VCH Verlag GmbH & Co. KGaA, Weinheim

their accessibility.[14] In this context, we propose herein the use of a DNA hybridization detection scheme based on atomic force microscopy (AFM) imaging using unlabeled DNA probes and targets adsorbed on a flat surface at low density. The method takes advantage of two different aspects:

1) The bioactive surface used is muscovite mica, a clay mineral that can withstand high temperatures. Its atomic flatness allows easy imaging of DNA molecules at high resolution, which explains its extensive use as a substrate for AFM imaging of nucleic acids[15] and DNA/protein complexes.[16] Beyond these advantages, a major interest of this surface for biosensor applications lies in the recent advances in the understanding of the mechanism of DNA adsorption on mica. It has been shown that the binding strength of DNA to the mica surface can be finely tuned by varying the relative concentration of multivalent cations used in the adsorption buffer.[17] Then, one can obtain weak electrostatic adsorption of DNA on mica, which is sufficient for quality imaging and which preserves DNA accessibility to ligands (proteins, drugs).[18] Furthermore, use of multivalent cations such as spermidine allows an easy distinction of both ssDNA and double-stranded DNA (dsDNA) on mica.[19]
2) The reliable detection of discrete DNA hybridization events is based on the measurement, in AFM images, of the contour length of single hybridized dsDNA adsorbed on mica. The AFM technique has proven its ability to detect DNA hybridization by using, for example, nanomechanical measurements.[20] Other approaches are based on topographical description,[21] such as changes in height (or roughness) of areas after hybridization[21f] or changes in self-assembled bare coded nucleic acid probe tiles.[21g] AFM generally prevents the use of any external labeling or enzymatic manipulations and the nanoscale detection scheme leads to low detection limits.

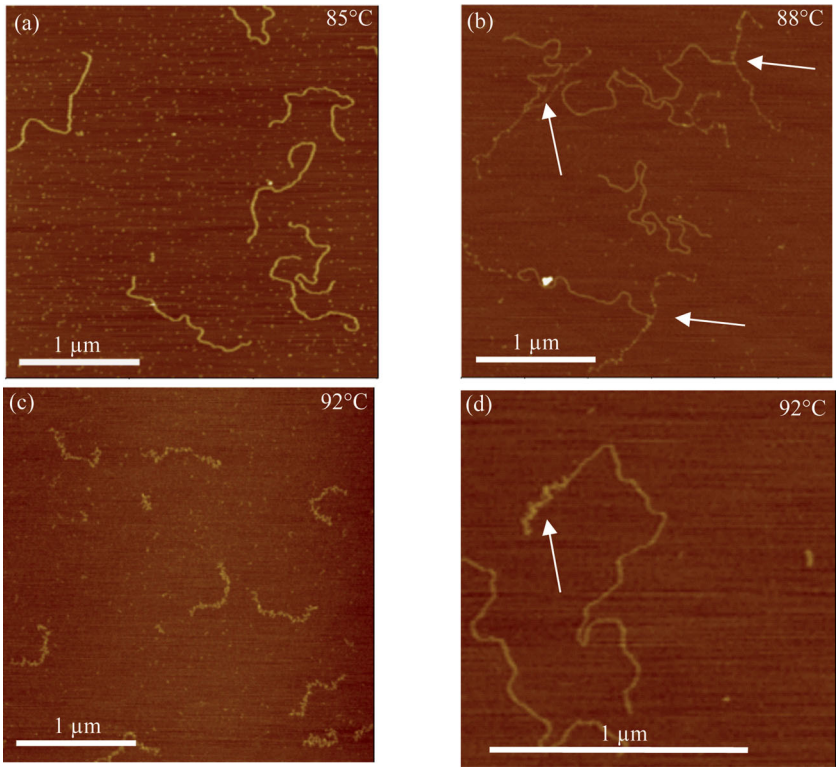

Figure 1. DNA denaturation on mica. AFM images (a–c) of linearized pBR322 adsorbed on a mica surface in 4 μM spermidine solution at varying denaturation temperatures as indicated. Image (d) was obtained with a denaturation solution comprising 20 mM Tris-HCl (pH 7.5), 50 mM NaCl, and 100 μM spermidine, incubated at 92 °C. Arrows in (b) and (d) point to the single-stranded portions of partially denatured DNA.

In the present study, we investigated the hybridization of ssDNA fragments adsorbed on mica. The hybridization mechanism first involves the facilitated diffusion of ssDNA strands on a mica surface leading to an encounter between two complementary ssDNA strands, and then hybridization resulting from molecular arrangements between the two complementary strands. Facilitated diffusion has already been introduced to explain how proteins can find their target by 1D sliding along long DNA molecules[22] or microtubules,[23] and can be extended to 2D diffusion on surfaces such as mica. We furthermore quantified the influence of incubation time, temperature, and ionic composition of the buffer on the probability of DNA hybridization. The effects of DNA length, molecular crowding, and incomplete hybridization were also considered, which provided important information on using this approach in more complex systems than a single couple "probe-target". Finally, we elaborated some practical interests regarding the potential development of this method in DNA biosensor technology.

2. Results

2.1. Denaturation and Adsorption of ssDNA on Mica at High Temperature

To generate isolated ssDNA molecules, dsDNA was first heated at high temperatures for 4 min in pure water containing 4 μM spermidine, before adsorption on a mica surface. The point is to determine the temperature required to observe only ssDNA molecules on mica in these particular ionic conditions (**Figure 1**).

When dsDNA was heated at 85 °C, it remained in the double-stranded state (Figure 1a). At 88 °C, the denaturation process was incomplete (Figure 1b), as previously reported by electron microscopy,[24] with long stretches of ssDNA clearly identifiable by AFM together with the nondenatured part of dsDNA. At 92 °C, the denaturation process was completed and all DNA molecules were in their single-stranded state and well separated from each other (Figure 1c). By increasing

© 2013 Wiley-VCH Verlag GmbH & Co. KGaA, Weinheim
small 2013,
DOI: 10.1002/smll.201300546

NANO MICRO small

the ionic strength of the buffer (100 μM spermidine, 50 mM NaCl), the melting of DNA shifted toward higher temperature (92 °C compared to 88 °C) due to weaker electrostatic repulsion between complementary strands (Figure 1d).

For the rest of this study, we performed DNA hybridization assays on mica following DNA adsorption at 95 °C in 4 μMspermidine, thus ensuring that all adsorbed molecules were isolated and in their single-stranded state. The interest of using spermidine is that DNA molecules can be adsorbed in the presence of a low concentration of this natural polyamine, thus allowing a clear distinction between the double- and single-stranded parts of adsorbed DNA. This cannot be obtained using Mg^{2+} since a three orders of magnitude higher concentration of this cation is required for DNA adsorption under similar conditions, and ssDNA would appear in a globular shape.[19]

2.2. Influence of Temperature, Counterions, and Time on Hybridization Efficiency on Mica

After denaturation and adsorption of DNA molecules, the mica surface was rinsed at 95 °C in 4 μM spermidine solution to remove unadsorbed fragments.

2.2.1. Effect of Hybridization Temperature

The mica was then incubated for 15 min in a magnesium-rich buffer (20 mM $MgCl_2$, 50 mM NaCl, 20 mM Tris-HCl pH 7.5) at varying temperatures to allow both DNA diffusion on the surface and hybridization of the complementary DNA strands. The results showed that DNA hybridization exhibits a typical pattern with an optimum hybridization temperature of about 65 °C (**Figure 2**a). Indeed, for the 1000 base pair (bp) DNA fragment, the surface density of the hybridized fragment was maximum at 65 °C. Reduction of the association probability at high temperature was related to the fact that the two complementary strands evolved in more stringent conditions. On the contrary, at temperatures lower than 65 °C, the increased probability of cross-hybridization processes reduced the surface density of fully hybridized fragments. Consequently, the next experiments were performed at 65 °C, a temperature classically used for DNA microarray experiments.[25]

2.2.2. Effect of Varying the Nature and Concentration of Multivalent Cations

We examined the impact of three multivalent cations, Mg^{2+}, putrescine (Pu^{2+}), and spermidine (Spd^{3+}), on the hybridization of ssDNA adsorbed on mica, owing to their known ability to favor DNA adsorption. Among these, magnesium leads to a weaker adsorption on mica than putrescine and spermidine, two natural divalent and trivalent polyamines, respectively. Indeed, polyamines are linear molecules that allow a closer approach between DNA and mica than does the globular magnesium.[26] In addition, spermidine induces a stronger adsorption than putrescine owing to its higher valency. We have shown recently that 20 mM $MgCl_2$, 2 mM

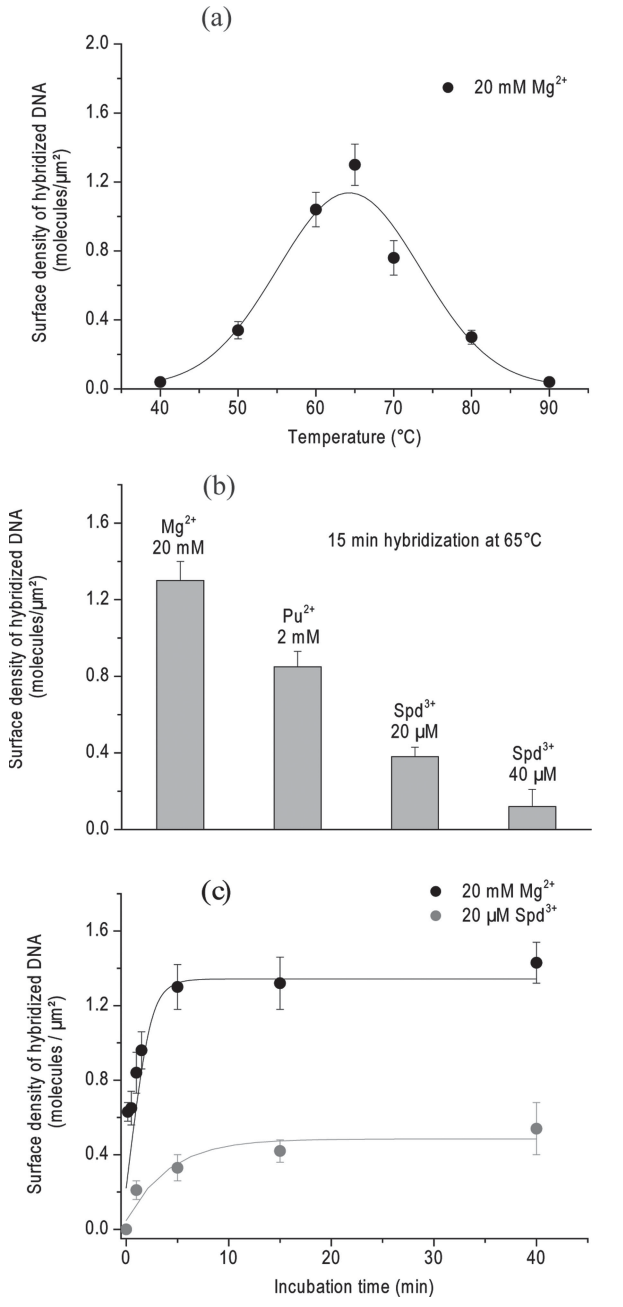

Figure 2. Experimental conditions that promote surface DNA hybridization. a) Surface density of hybridized 1000 bp DNA on a mica surface after 15 min of incubation in 20 mM Tris-HCl (pH 7.5), 50 mM NaCl, 20 mM $MgCl_2$ at different temperatures. The maximum value of hybridization efficiency occurs at 65 °C. b) Surface density of hybridized 1000 bp DNA on a mica surface after 15 min of incubation at 65 °C in 20 mM Tris-HCl (pH 7.5), 50 mM NaCl, with varying multivalent cations ($MgCl_2$, putrescine (Pu^{2+}), or spermidine (Spd^{3+})). The cation valence is not the unique parameter to be considered for hybridization as both the geometry (globular or linear) and ability to interact strongly with DNA and/or mica also come into play. c) Surface density of hybridized 1000 bp DNA on a mica surface after different incubation times at 65 °C in 20 mM Tris-HCl (pH 7.5), 50 mM NaCl, containing 20 mM $MgCl_2$ (black circles) or 20 μM spermidine (gray circles). Spermidine led to a stronger DNA adsorption on mica, which limits DNA strand diffusion and thus the probability of complete hybridization. When Mg^{2+} counterions are used to adsorb DNA on the mica surface, the maximum efficiency of hybridization is reached after only 5 min of incubation.

DOI: 10.1002/smll.201300546
© 2013 Wiley-VCH Verlag GmbH & Co. KGaA, Weinheim

Pu^{2+}, or 20 μM Spd^{3+} are sufficient to induce DNA adsorption on mica in the presence of 50 mM NaCl.[18] Monovalent salt (50 mM NaCl) was added to the buffer (20 mM Tris-HCl, pH 7.5) to reduce the adsorption strength, since monovalent cations partially replace multivalent cations on both the DNA and mica surfaces. We observed that hybridization is inversely related to adsorption strength. Indeed, the surface density of hybridized 1000 bp DNA increased in the following order: 40 μM Spd^{3+}, 20 μM Spd^{3+}, 2 mM Pu^{2+}, and the maximum was obtained with 20 mM $MgCl_2$ (Figure 2b). We thus concluded that increasing the adsorption strength is an unfavorable condition for surface hybridization on mica, as this lowered the hybridization rates and favored the formation of multiplexes or partial hybridization.

2.2.3. Effect of Incubation Time

The influence of incubation time on the hybridization efficiency was assessed in 20 mM Tris-HCl (pH 7.5), 50 mM NaCl with either 20 mM $MgCl_2$ or 20 μM Spd^{3+}. We noticed that the surface density of hybridized fragments increased with the incubation time up to 5 min and then reached a plateau value, which is lower when Spd^{3+} is used (Figure 2c). At incubation times shorter than 5 min, fully hybridized DNA, ssDNA, and partially hybridized ssDNA multiplexes were observed whereas beyond 5 min of incubation, isolated ssDNA fragments disappeared. Consequently, they were either transformed into fully hybridized DNA (80% of the adsorbed bodies) or partially hybridized DNA (20%, Supporting Information S3).

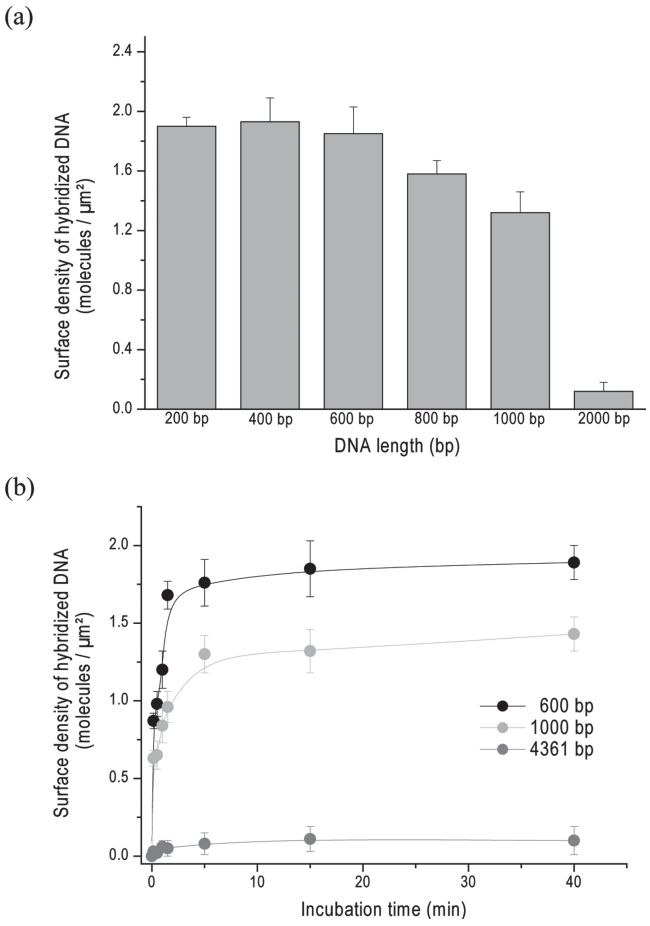

Figure 3. Influence of DNA length on the hybridization efficiency. a) DNA hybridization for various fragment lengths (200, 400, 600, 800, 1000, and 2000 bp). Hybridization was performed on a mica surface after 15 min of incubation at 65 °C in 20 mM Tris-HCl (pH 7.5), 50 mM NaCl, 20 mM $MgCl_2$. b) Detection of DNA hybridization for different incubation times in the same buffer as (a) and for different fragment lengths (600, 1000 bp, and pBR322).

2.3. Effect of Fragment Length on Hybridization Efficiency; Possibility of Detecting Different Probes on a Single Mica Surface

We compared the efficiency of surface hybridization for DNA fragments with different lengths ranging from 200 to 2000 bp in magnesium buffer (20 mM $MgCl_2$, 20 mM Tris-HCl (pH 7.5), 50 mM NaCl) at 65 °C. The results show that beyond 600 bp, the fragments were less likely to be hybridized on mica than shorter ones (**Figure 3**a). Interestingly, the fragment length has little influence on the time lag required to reach the maximum hybridization efficiency (5 min of incubation at 65 °C, Figure 3b).

As the present strategy potentially allows the simultaneous use of several probes on the same surface, we assessed the reliability of the detection scheme in the presence of five DNA fragments varying from 230 to 4361 bp, produced by the simultaneous digestion of pBR322 by a mixture of restriction enzymes, to have for each DNA fragment exactly the same number of molecules. DNA fragments were then denatured, adsorbed on mica, and allowed to hybridize for 15 min in magnesium buffer at 65 °C. The length distribution of adsorbed dsDNA before denaturation exhibited narrow peaks, each of which corresponded to a single dsDNA fragment (**Figure 4**a). We then denatured the five DNA fragments at 95 °C and allowed them to hybridize simultaneously on the same mica sample. Interestingly, we observed under these conditions the appearance of five peaks, the positions of which match the five peaks found with the double-stranded fragments (Figure 4b). Consequently, as long as the DNA length was shorter than 400 nm (about 1200 bp), the width of the peak distribution corresponded to the experimental error, that is, about ±10 nm. However, for DNA lengths higher than 400 nm, the peak of the hybridized product appears broader. For example, the 700 nm fragments led to a larger length distribution, ranging from 500 to 750 nm, which was most likely due to partial hybridization. This indicated that the present detection scheme is not valid for DNA molecules longer than 400 nm. Concerning the lower limit of the DNA length, the hybridization of a 78 nm (230 bp) long DNA fragment was still clearly detectable (Figure 4c and d).

2.4. Influence of Crowded Environment on Surface Hybridization and Accuracy of the Detection Method

DNA microarray or biosensor experiments are often used to evidence the presence of a nucleic acid fragment in a complex

© 2013 Wiley-VCH Verlag GmbH & Co. KGaA, Weinheim

DOI: 10.1002/smll.201300546

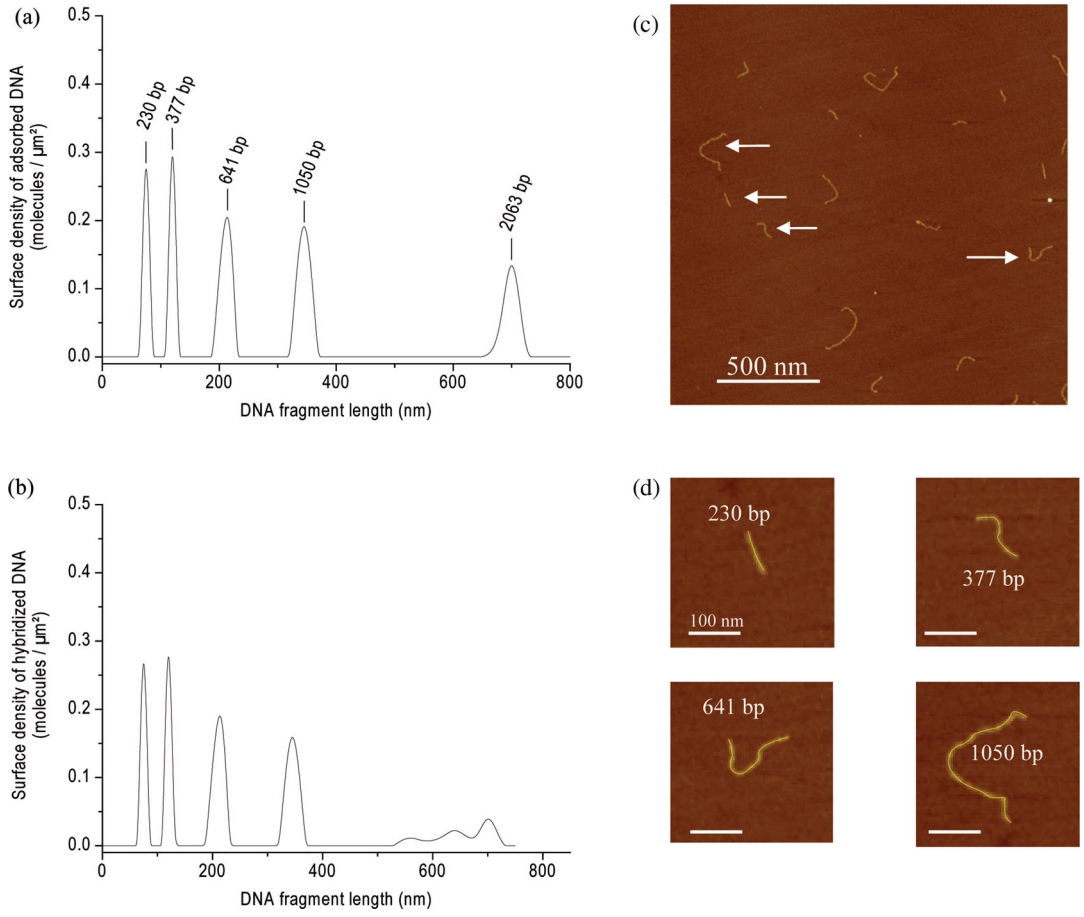

Figure 4. Simultaneous hybridization of different DNA fragments. a) Surface density of 230 bp (78 ± 15 nm), 377 bp (128 ± 15 nm), 641 bp (217 ± 15 nm), 1050 bp (357 ± 15 nm), and 2063 bp (702 ± 15 nm) dsDNA simultaneously adsorbed on a mica surface without any denaturation step. b) The same series of DNA was denatured at 95 °C, adsorbed, and then allowed to hybridize on mica in 20 mM Tris-HCl (pH 7.5), 50 mM NaCl, 20 mM $MgCl_2$ for 15 min at 65 °C. Interestingly, the peak widths of the DNA fragment length distribution in (a) correspond to that expected owing to the AFM resolution. In (b), for the dsDNA fragments shorter than about 400 nm (i.e., 1200 bp) the peak width after the hybridization process is identical to that obtained without denaturation. c) AFM image of DNA molecules adsorbed on mica after the hybridization process and d) zoom views on fragments having different lengths.

analyte mixture containing a wealth of other fragments. To mimic these conditions, various amounts of a 600 bp fragment were denatured and then hybridized on a mica surface in the magnesium buffer in the presence of a fixed amount of M13mp18 ssDNA (**Figure 5**a). We observed that the 600 bp hybridization is progressively reduced when increasing the [M13]/[600 bp] molar ratio. However, the detection of hybridized 600 bp was still possible even at low concentration by adjusting the scan area (Figure 5b). Notably, in this experiment, the molar concentration of the 600 bp target ranged

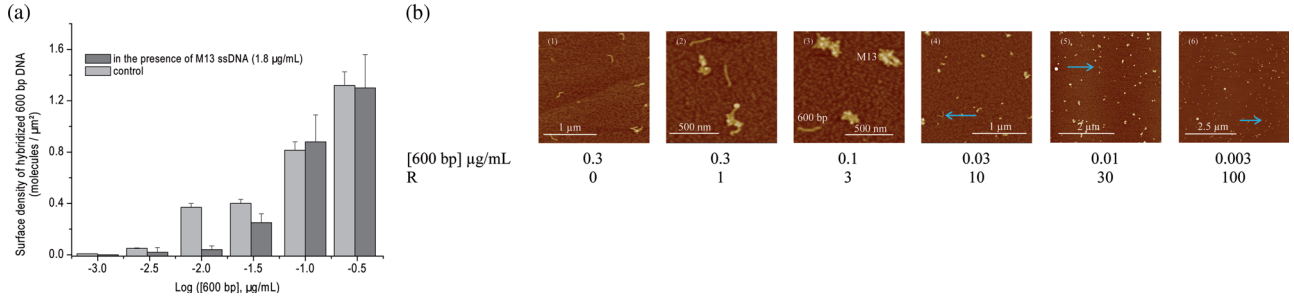

Figure 5. Effect of an excess of noncomplementary DNA fragments on 600 bp surface hybridization. a) Surface density of hybridized 600 bp DNA on mica after 15 min of incubation at 65 °C in 20 mM Tris-HCl (pH 7.5), 50 mM NaCl, 20 mM $MgCl_2$ in the presence of 1.8 µg mL^{-1} M13mp18 ssDNA. M13 ssDNA and various concentrations of denatured 600 bp DNA were adsorbed simultaneously on mica at 95 °C followed by surface hybridization at 65 °C. The molar ratio, R = [M13]/[600 bp] varied from 1 to 300. b) AFM images of DNA molecules (600 bp alone in (1) or both 600 bp and M13 in (2–6)) after the hybridization process as described previously. Arrows indicate the presence of hybridized 600 bp for high R values.

DOI: 10.1002/smll.201300546
© 2013 Wiley-VCH Verlag GmbH & Co. KGaA, Weinheim

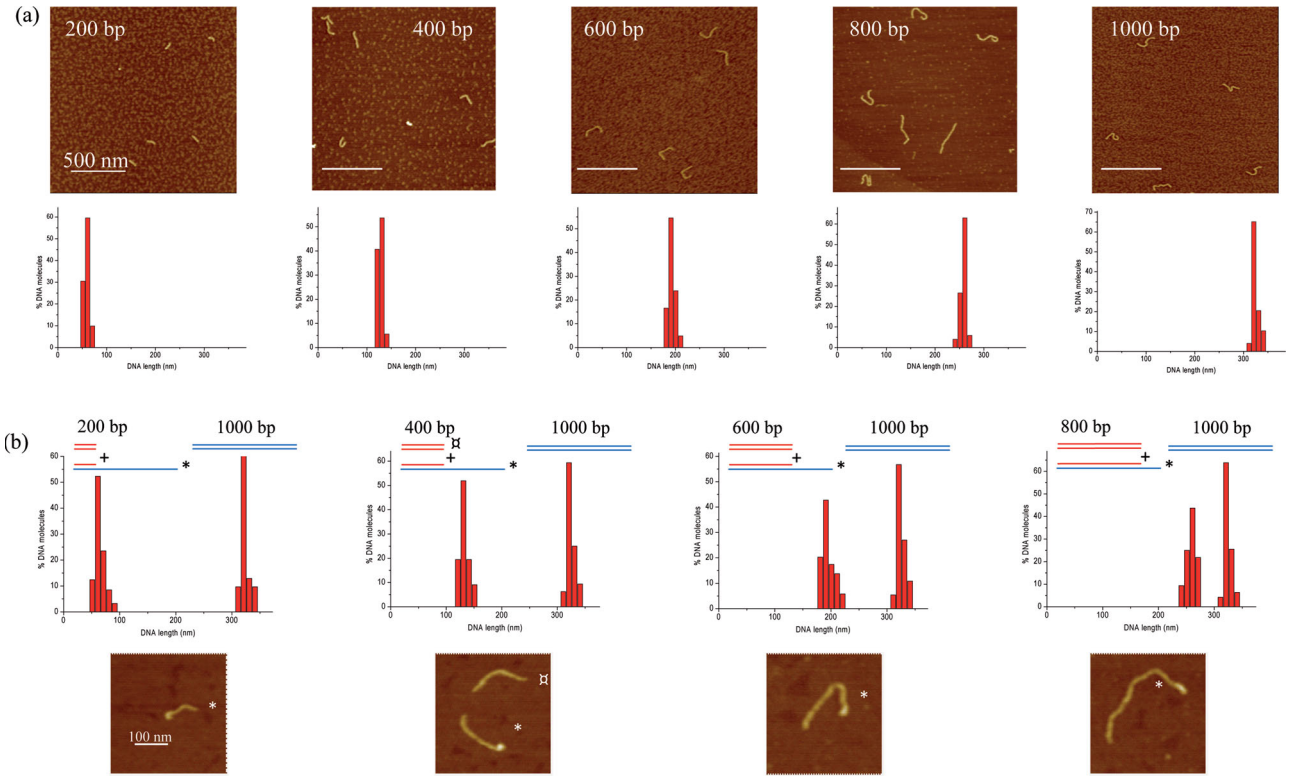

Figure 6. Influence of noncomplementary ssDNA fragment length on the accuracy of the contour length measurement. a) AFM images and contour length measurements of 200, 400, 600, 800, and 1000 bp fragments after denaturation at 95 °C followed by surface hybridization in 20 mM Tris-HCl (pH 7.5), 50 mM NaCl, 20 mM $MgCl_2$ for 15 min at 65 °C. As expected, the contour length is measured with an accuracy of ±10 nm, whatever the fragment length. b) Same as (a) but the denaturation and hybridization processes are done with mixing 200, 400, 600, and 800 bp fragments with a complementary 1000 bp DNA, and thus cross-hybridization could occur. These cross-hybridizations induce a slight enlargement of the length distribution histograms but the measurement of the fragment lengths remains reliable with an accuracy of ±20 nm. In AFM images, the ssDNA part of the fragment is easily detected due to the formation of a small dot at one end.

from nanomoles to picomoles, that is, like the practical target concentration detected by DNA biosensors.

When the target and probe are complementary and have the same length, the detection of hybridization by fragment length measurement is limited to the AFM tip resolution (**Figure 6**a). However, for biosensor applications, probes and targets often differ in length and the point is to determine whether the single-stranded part of the partially hybridized fragment could be detected. To that end, we prepared different couples of ssDNA fragments that are complementary over only a part of their length. This was achieved by mixing a 1000 bases ssDNA fragment with complementary ssDNA of 200, 400, 600, or 800 base length. We observed in each case that the contour length measurement error was slightly broadened by ±10 nm maximum (Figure 6b), which would not appear as an obstacle for the detection of short oligonucleotide hybridization on a long DNA fragment. Interestingly, the single-stranded part on the DNA fragment was clearly detected as a small bright dot at one of its ends and appeared in the AFM images.

3. Discussion

To assess DNA hybridization at the single-molecule level, we propose a novel detection scheme based on the measurement of DNA contour length by AFM. A key point is the choice of the substrate on which DNA targets and probes are adsorbed, as the detection scheme requires the spreading of targets and probes with no impairment of their hybridization ability. Mica was used as a substrate for this purpose since DNA adsorption on it is mediated by multivalent cations and thus can be controlled by varying the ionic composition of the buffer to favor DNA accessibility and its diffusion on the surface. In this context, Mg^{2+} induces a very weak adsorption and thus appears to be a good candidate. To further modulate the DNA binding to mica, a monovalent salt can be added since the replacement of magnesium counterions by monovalent ones on both DNA and mica surfaces weakens DNA adsorption. A good compromise has been found with the following buffer: 20 mM $MgCl_2$, 20 mM Tris-HCl (pH 7.5), 50 mM NaCl, which combines weak binding and quasi-irreversible adsorption during the incubation step (less than 1 h).

The major interest of using loosely adsorbed DNA is that DNA diffusion on the surface allows both the decrease of density of the probe on the surface and the incubation time necessary for the hybridization step. This potential interest has already been reported as hybridization could occur after an initial nonspecific adsorption step of the target followed by surface diffusion to the probe.[27] The rate of hybridization per unit area is an increasing function of the surface diffusion

© 2013 Wiley-VCH Verlag GmbH & Co. KGaA, Weinheim
small 2013,
DOI: 10.1002/smll.201300546

NANO MICRO small

of the target DNA. However, for a small distance (a few μm) between neighboring probes, facilitated diffusion does not increase further the rate of the hybridization process. As the probe densities in oligonucleotide chips vary between 2 and 6×10^{12} strands cm^{-2},[12] the distance separating neighboring probes is around a few nanometers, which means that the potential use of surface diffusion cannot really be exploited. Here, our aim is rather to detect hybridization with a very low density of probes by using AFM while keeping a high sensitivity of detection. In this case, surface diffusion of DNA molecules becomes mandatory to increase the rate of hybridization. To illustrate this point, let us use a simple model that describes the influence of DNA diffusion on the mica surface on incubation time. In a previous study,[28] we reported that the diffusion constant (D) of 400-nm-long DNA molecules on mica under loose adsorption conditions is about 9.10^{-15} m^2 s^{-1}. If we consider that under the conditions used in this study (except for Figure 5) the mean separation distance between probes and targets is about 2 μm, the encounter between probes and targets can occur after an incubation time of about 3 min, which is in agreement with the present experimental results (Figures 2c and 3b). The reaction is then rather rapid even for such a low DNA surface density.

Another point of interest is that the DNA probes and targets evolve in the same environment relative to the surface. This is not the case for probes anchored to the substrate, for which strand reactivity depends on the distance from the substrate. Indeed, numerous studies have evidenced that when the length of the target does not match that of the probe, up to hundreds of bases, the presence of the substrate could introduce a bias in the hybridization efficiency.[14,29] In this case, the noncomplementary part of the target may be oriented toward the substrate, which may induce steric hindrance with a reported decrease of the hybridization efficiency by more than 50%.[11,30]

Besides the interest in fundamental research concerning DNA accessibility and its surface diffusion, the practical advantage of the present method relies on its putative application in DNA biosensor technologies. Indeed, we demonstrated that tiny amounts of unlabeled nucleic acids (a few nanograms, see Experimental Section) could be detected at the single-molecule level at the nanometer scale and with a discrete response at the monomolecular level (nonhybridized or hybridized molecules). This is completely different from optic-based technologies, for which detection of hybridization is based on the mean value of the optical signal measured over a large number of molecules.

However, several points have to be clarified before the practical use of this method in the DNA biosensor field. Among these, the sensitivity of the method in the presence of few mismatches between probes and target has to be established. A better understanding of the relationships between the surface density of hybridized nucleic acids on mica surfaces and target concentration also remains to be explored. However, the promise of the present method in the DNA biosensor domain deserves further investigations.

Table 1. List of the different dsDNA fragments generated by PCR used in this study.

Primers	Orientation	Synthesized fragment length [bp]	Name of the fragment
5′-CGCGCGTTTCGGTGATG-3′	forward		
5′-GTGCGGTATTTCACACCG-3′	reverse	205	200 bp
5′-GCTCGAATTCACTGGCCG-3′	reverse	404	400 bp
5′-GGGCAGTGAGCGCAACGC-3′	reverse	599	600 bp
5′-CTTTCCTGCGTTATCCCC-3′	reverse	803	800 bp
5′-GTCGGAACAGGAGAGCGC-3′	reverse	1000	1000 bp
5′-CGTTGGGAACCGGAGCTG-3′	reverse	2002	2000 bp

4. Experimental Section

DNA Fragments: Chemical compounds ($MgCl_2$, putrescine, spermidine), pBR322, and M13mp18 phage ssDNA were purchased from Sigma–Aldrich. Restriction enzymes were purchased from Sigma–Aldrich (PvuII, EcoRV) or New England Biolabs (EcoRI, BamHI, NdeI, and BsoBI).

To generate dsDNA fragments of different sizes (205, 404, 599, 803, 1000, and 2002 bp) by the polymerase chain reaction (PCR), we used the pUC19 plasmid as a template, a unique forward primer and a series of specific reverse primers (see **Table 1** for primers and products). The PCR products were run on 1% agarose gel and purified using a gel extraction kit from Fermentas. The purified DNA samples were resuspended in water.

The 230, 377, 641, 1050, and 2063 bp DNA fragments were obtained by simultaneous digestion of pBR322 with a mix of restriction endonuclease (EcoRI, BamHI, BsoBI, PvuII, and NdeI) in NEBuffer II. The linear 4361 bp fragment was obtained by pBR322 digestion with EcoRV.

Atomic Force Microscopy: Sample imaging was performed in Tapping Mode with a Multimode AFM instrument (Veeco, Santa Barbara, CA) operating with a Nanoscope IIIa controller. We used Olympus (Hamburg, Germany) silicon cantilevers AC160TS with resonant frequencies of about 300 kHz and nominal spring constants between 10 and 100 N m^{-1}. The scan frequency was typically 1.5 Hz per line and the modulation amplitude was about a few nanometers. Data were acquired at a set point chosen to minimize tip–sample interaction. Image analysis was performed using the Nanoscope IIIa software. We only used a first- or second-order polynomial function to remove the background.

Experimental Procedure to Detect DNA Hybridization on Mica: We chose an initial DNA concentration sufficiently low (7.6×10^{-10} M) to limit the formation of multiplexes during the hybridization step (see Supporting Information Figure S2). The dsDNA fragment was first denatured at 95°C in 4 μM spermidine solution (300 μL) for 4 min, thus leading to a solution containing both complementary strands at equimolar concentration (**Scheme 1**a). A freshly cleaved mica surface (0.5×1.5 cm^2), heated to be at the same temperature in a dry atmosphere, was plunged into the DNA solution during 40 s to adsorb the complementary fragments of ssDNA (Scheme 1b). For practical reasons, a large piece of mica (0.75 cm^2) and thus a large volume of DNA solution (300 μL) were used in this study. However, for future developments, a significantly smaller area (a few hundred μm^2 per spot), on which a few

DOI: 10.1002/smll.201300546
© 2013 Wiley-VCH Verlag GmbH & Co. KGaA, Weinheim

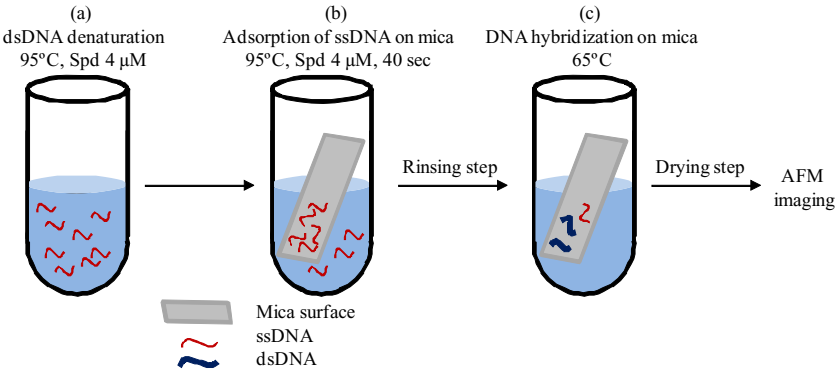

Scheme 1. Experimental process. DNA fragments were denatured at 95 °C for 4 min in a 4 μM spermidine (Spd) solution (a). A mica surface was dipped into the DNA solution at 95 °C during 40 s to adsorb ssDNA fragments (b). It was then incubated in a large volume of 4 μM spermidine solution at 95 °C to remove unadsorbed fragments. For hybridization between the complementary strands, the surface was plunged in 20 mM Tris-HCl (pH 7.5), 50 mM NaCl containing different concentrations of multivalent counterions at lower temperature (c). The hybridization process was stopped by rinsing the mica with uranyl acetate solution.

microliters of DNA solution can be deposited (a few nanograms of DNA per spot), could be used.

After a rinsing step with a 4 μM spermidine solution at same temperature to remove unabsorbed ssDNA fragments, the mica surface was directly plunged in buffer (500 μL) containing 20 mM Tris-HCl (pH 7.5), 50 mM NaCl and different concentrations of divalent ($MgCl_2$, putrescine) or trivalent counterions (spermidine). Hybridization between the complementary fragments adsorbed on the mica surface was then allowed to take place for different periods of time (Scheme 1c). A low surface density of adsorbed ssDNA (about four ssDNA molecules μm^{-2}) was chosen to allow the detection of single hybridization events. The separation distance between two nearest ssDNA molecules should thus be larger than the radius of gyration of the hybridized DNA to avoid their overlapping (distances larger than 200 nm for a 4000 bp plasmid).

After varying incubation periods, the mica surface was rinsed with 0.02% uranyl acetate solution to stop the hybridization process and to stabilize the DNA molecules in their conformations for AFM imaging in air.[31] The sample was then rinsed rapidly with pure water (Millipore) and dried with filter paper to obtain a clean surface for AFM imaging.

Control Experiment: We first explored whether DNA molecules could be released from the mica surface into the solution during the hybridization period. We thus performed the ssDNA adsorption and hybridization as described above and then removed the mica surface on which DNA molecules were adsorbed and potentially hybridized. A control mica surface was then plunged into this incubation buffer to which we added 100 μM spermidine to enhance DNA adsorption. After 10 min of incubation, we observed by AFM whether or not putative desorbed DNA molecules could be reabsorbed on the control mica. The results clearly indicated that no DNA molecule was detected on the control mica. Consequently, desorption did not occur during the hybridization experiments on mica under the conditions reported herein, in agreement with our previous results.[18] To certify the absence of DNA desorption from the surface, we also observed that the surface density of hybridized DNA remained constant whatever the incubation time.

Identification Criterion of the Hybridization Efficiency (Figure S3): We evaluated the efficiency of hybridization by the surface density of completely hybridized molecules. First, nonhybridized DNA (ssDNA) and multimolecular aggregates due to cross hybridization were discarded for this analysis. ssDNA fragments were clearly distinguished on AFM images (Figure S1). To analyze properly the population of hybridized molecules, we chose to measure on AFM images the contour length of the hybridized fragments. We considered a probe/target complex to be fully hybridized when the length of the complex was equal to the theoretical value of the two fully hybridized molecules (number of base pair × 0.34 ± 10 nm). The DNA length was measured with an accuracy of ±10 nm using the ImageJ software. For each data point, three different mica samples were analyzed and at least 100 DNA molecules were measured from each surface. We report here the mean value of the surface density of hybridized molecules obtained for the three mica samples, which corresponds to more than 200 hybridization events.

Supporting Information

Supporting Information is available from the Wiley Online Library or from the author.

Acknowledgements

We gratefully acknowledge the Genopole Evry for constant support of the laboratory. This work was supported by INSERM.

[1] A. Sassolas, B. D. Leca-Bouvier, L. J. Blum, *Chem. Rev.* **2008**, *108*, 109–139.
[2] a) R. J. Lipshutz, S. P. Fodor, T. R. Gingeras, D. J. Lockhart, *Nat. Genet.* **1999**, *21*, 20–24; b) A. Halperin, A. Buhot, E. B. Zhulina, *Langmuir* **2006**, *22*, 11290–11304; c) G. Ramsay, *Nat. Biotechnol.* **1998**, *16*, 40–44.
[3] a) J. Lu, G. Getz, E. A. Miska, E. Alvarez-Saavedra, J. Lamb, D. Peck, A. Sweet-Cordero, B. L. Ebert, R. H. Mak, A. A. Ferrando, J. R. Downing, T. Jacks, H. R. Horvitz, T. R. Golub, *Nature* **2005**, *435*, 834–838; b) C. Chen, W. Wang, J. Ge, X. S. Zhao, *Nucleic Acids Res.* **2009**, *37*, 3756–3765; c) B. A. Baker, V. T. Milam, *Nucleic Acids Res.* **2011**, *39*, e99.
[4] a) C. Heise, F. F. Bier in *Immobilization of DNA on Microarrays*, *Vol. 261*, Springer, Berlin, **2005**, pp. 1–25; b) M. Dufva, *Biomol. Eng.* **2005**, *22*, 173–184; c) R. J. Lipshutz, S. P. A. Fodor, T. R. Gingeras, D. J. Lockhart, *Nat. Genet.* **1999**, *21*, 20–24.
[5] M. Schena, D. Shalon, R. W. Davis, P. O. Brown, *Science* **1995**, *270*, 467–470.
[6] a) T. G. Drummond, M. G. Hill, J. K. Barton, *Nat. Biotechnol.* **2003**, *21*, 1192–1199; b) C. Fan, K. W. Plaxco, A. J. Heeger, *Proc. Natl.*

© 2013 Wiley-VCH Verlag GmbH & Co. KGaA, Weinheim

DOI: 10.1002/smll.201300546

Acad. Sci. USA **2003**, *100*, 9134–9137; c) S. J. Park, T. A. Taton, C. A. Mirkin, *Science* **2002**, *295*, 1503–1506.

[7] a) R. Gabl, H. D. Feucht, H. Zeininger, G. Eckstein, M. Schreiter, R. Primig, D. Pitzer, W. Wersing, *Biosens. Bioelectron.* **2004**, *19*, 615–620; b) F. Caruso, E. Rodda, D. N. Furlong, K. Niikura, Y. Okahata, *Anal. Chem.* **1997**, *69*, 2043–2049.

[8] a) J. L. Arlett, E. B. Myers, M. L. Roukes, *Nat. Nanotechnol.* **2011**, *6*, 203–215; b) R. McKendry, J. Zhang, Y. Arntz, T. Strunz, M. Hegner, H. P. Lang, M. K. Baller, U. Certa, E. Meyer, H. J. Guntherodt, C. Gerber, *Proc. Natl. Acad. Sci. USA* **2002**, *99*, 9783–9788.

[9] a) T. Livache, E. Maillart, N. Lassalle, P. Mailley, B. Corso, P. Guedon, A. Roget, Y. Levy, *J. Pharm. Biomed. Anal.* **2003**, *32*, 687–696; b) L. Song, S. Ahn, D. R. Walt, *Anal. Chem.* **2006**, *78*, 1023–1033; c) X. Zhou, J. Zhou, *Anal. Chem.* **2004**, *76*, 5302–5312.

[10] D. Horejsh, F. Martini, F. Poccia, G. Ippolito, A. Di Caro, M. R. Capobianchi, *Nucleic Acids Res.* **2005**, *33*, e13.

[11] a) D. S. Dandy, P. Wu, D. W. Grainger, *Proc. Natl. Acad. Sci. USA* **2007**, *104*, 8223–8228; b) K. B. Cederquist, C. D. Keating, *Langmuir* **2010**, *26*, 18273–18280.

[12] A. W. Peterson, R. J. Heaton, R. M. Georgiadis, *Nucleic Acids Res.* **2001**, *29*, 5163–5168.

[13] a) K. Castelino, B. Kannan, A. Majumdar, *Langmuir* **2005**, *21*, 1956–1961; b) Y. Zu, Z. Gao, *Anal. Chem.* **2009**, *81*, 8523–8528.

[14] a) S. R. Nicewarner Pena, S. Raina, G. P. Goodrich, N. V. Fedoroff, C. D. Keating, *J. Am. Chem. Soc.* **2002**, *124*, 7314–7323; b) X. Bin, E. H. Sargent, S. O. Kelley, *Anal. Chem.* **2010**, *82*, 5928–5931.

[15] Y. L. Lyubchenko, L. S. Shlyakhtenko, T. Ando, *Methods* **2011**, *54*, 274–283.

[16] a) D. J. Billingsley, W. A. Bonass, N. Crampton, J. Kirkham, N. H. Thomson, *Phys. Biol.* **2012**, *9*, 021001; b) A. J. Katan, C. Dekker, *Cell* **2011**, *147*, 979–982; c) P. A. Sontz, T. P. Mui, J. O. Fuss, J. A. Tainer, J. K. Barton, *Proc. Natl. Acad. Sci. USA* **2012**, *109*, 1856–1861.

[17] D. Pastré, L. Hamon, F. Landousy, I. Sorel, M. O. David, A. Zozime, E. Le Cam, O. Pietrement, *Langmuir* **2006**, *22*, 6651–6660.

[18] D. Pastre, L. Hamon, I. Sorel, E. Le Cam, P. A. Curmi, O. Pietrement, *Langmuir* **2010**, *26*, 2618–2623.

[19] L. Hamon, D. Pastre, P. Dupaigne, C. Le Breton, E. Le Cam, O. Pietrement, *Nucleic Acids Res.* **2007**, *35*, e58.

[20] a) L. T. Mazzola, C. W. Frank, S. P. Fodor, C. Mosher, R. Lartius, E. Henderson, *Biophys. J.* **1999**, *76*, 2922–2933; b) J. Wang, A. J. Bard, *Anal. Chem.* **2001**, *73*, 2207–2212; c) S. Husale, H. H. Persson, O. Sahin, *Nature* **2009**, *462*, 1075–1078.

[21] a) E. Casero, M. Darder, D. J. Diaz, F. Pariente, J. A. Martin-Gago, H. Abruna, E. Lorenzo, *Langmuir* **2003**, *19*, 6230–6235; b) M. H. Rouillat, V. Dugas, J. R. Martin, M. Phaner-Goutorbe, *Appl. Surf. Sci.* **2005**, *252*, 1765–1771; c) A. Nabok, A. Tsargorodskaya, D. Gauthier, F. Davis, S. P. Higson, T. Berzina, L. Cristofolini, M. P. Fontana, *J. Phys. Chem. B* **2009**, *113*, 7897–7902; d) C. G. Evans, R. F. Hariadi, E. Winfree, *J. Am. Chem. Soc.* **2012**; e) D. Zhou, K. Sinniah, C. Abell, T. Rayment, *Angew. Chem. Int. Ed.* **2003**, *42*, 4934–4937; f) F. Cattaruzza, A. Cricenti, A. Flamini, M. Girasole, G. Longo, T. Prosperi, G. Andreano, L. Cellai, E. Chirivino, *Nucleic Acids Res.* **2006**, *34*, e32; g) Y. Ke, S. Lindsay, Y. Chang, Y. Liu, H. Yan, *Science* **2008**, *319*, 180–183.

[22] a) O. G. Berg, R. B. Winter, P. H. von Hippel, *Biochemistry* **1981**, *20*, 6929–6948; b) R. B. Winter, O. G. Berg, P. H. von Hippel, *Biochemistry* **1981**, *20*, 6961–6977.

[23] A. Mechulam, K. G. Chernov, E. Mucher, L. Hamon, P. A. Curmi, D. Pastre, *PLoS Comput. Biol.* **2009**, *5*, e1000255.

[24] Y. A. Kalambet, A. S. Borovik, V. I. Lyamichev, Y. L. Lyubchenko, *Biopolymers* **1985**, *24*, 359–377.

[25] M. Schena in *DNA Microarrays: A Practical Approach*, *Vol. 205*, (Ed: B. D. Hames), Oxford University Press, Oxford, **1999**

[26] I. Rouzina, V. A. Bloomfield, *Biophys. J.* **1998**, *74*, 3152–3164.

[27] a) V. Chan, D. J. Graves, S. E. McKenzie, *Biophys. J.* **1995**, *69*, 2243–2255; b) D. Erickson, D. Q. Li, U. J. Krull, *Anal. Biochem.* **2003**, *317*, 186–200; c) I. Y. Wong, N. A. Melosh, *Biophys. J.* **2010**, *98*, 2954–2963.

[28] D. Pastre, O. Pietrement, A. Zozime, E. Le Cam, *Biopolymers* **2005**, *77*, 53–62.

[29] R. D. Stedtfeld, L. M. Wick, S. W. Baushke, D. M. Tourlousse, A. B. Herzog, Y. Xia, J. M. Rouillard, J. A. Klappenbach, J. R. Cole, E. Gulari, J. M. Tiedje, S. A. Hashsham, *Appl. Environ. Microbiol.* **2007**, *73*, 380–389.

[30] J. Zhang, R. Lao, S. Song, Z. Yan, C. Fan, *Anal. Chem.* **2008**, *80*, 9029–9033.

[31] B. Revet, A. Fourcade, *Nucleic Acids Res.* **1998**, *26*, 2092–2097.

Received: February 20, 2013
Published online:

© 2013 Wiley-VCH Verlag GmbH & Co. KGaA, Weinheim